CHIN. PHYS. LETT. Vol. 38, No. 3 (2021) 032301

Quantum Anti-Zeno Effect in Nuclear β Decay

Ming Ji(姬明) and Chang Xu(许昌)*

School of Physics, Nanjing University, Nanjing 210093, China

(Received 14 October 2020; accepted 1 February 2021; published online 2 March 2021)

The acceleration of decay induced by frequency measurements, namely the quantum anti-Zeno effect (AZE), was first predicted by Kofman and Kurizki [Nature 405 (2000) 546]. The effect of the frequency measurements on nuclear β decay rate is analyzed based on the time-dependent perturbation theory. We present a detailed calculation of the decay rates of ^{3}H, ^{60}Co (β^- type), ^{22}Na, ^{106}Ag (β^+ type) and ^{18}F, ^{57}Co and ^{111}Sn (EC type) under frequency measurements. It is found that the effects of frequency measurements on the decay rates of β^+ and β^- cases are different from the case of EC, and the smaller the β decay energy is, the more favorable it is to observe the AZE in experiment. Based on our analysis, it is suggested that possible experimental candidates should have a small decay energy and a reasonable half life (such as ^{3}H) for observing the AZE in β decay.

DOI: 10.1088/0256-307X/38/3/032301

The deviation from the exponential decay of an unstable quantum state for short time causes the decay rate to be modified under frequency measurements.[1–4] Therefore, if the frequency measurements inhibit the evolution of an unstable quantum state, this peculiar phenomenon can be called the quantum Zeno effect (QZE).[5–12] The inhibitory effect of QZE has attracted much theoretical and experimental interests, which has been used to cool down and to purify a quantum system,[13] to protect quantum information,[14] and to preserve quantum coherence and entanglement,[15,16] etc. However, an enhancement of the evolution may also occur due to the frequency measurements, namely quantum anti-Zeno effect (AZE).[17–22]

The QZE was successfully observed in a number of experiments. For example, in the experiment of Bose–Einstein condensates,[23] the continuous and pulsed quantum Zeno effects were observed using an ^{87}Rb Bose–Einstein condensate. Another example was discussed in Refs. [24–26], the quantum Zeno effect was demonstrated experimentally by suppressing the microwave-driven coherent spin dynamics between two ground-state spin levels of a single nitrogen vacancy center in diamond. In addition, the AZE was also successfully observed in many experiments. Take the experiment of trapped atoms as an example,[27] the decay of the cold sodium atoms, which were trapped by a detuned standing wave of light and could decay via a tunneling process, would be inhibited or enhanced when the measurements were performed during the initial period of non-exponential decay with different frequencies of measurements. Another example is the system of a nanomechanical oscillator,[28] in which the crossovers of QZE and AZE were observed by changing the system parameters such as the energy cutoff, oscillator frequency and bias voltage, etc.

The AZE was also possible in nuclear β decay.[29] The interaction involved in β decay is weak compared with the interaction that forms the quasi-stationary states, and the half-lives of β decay (typically in order of seconds or even years) are far longer than the characteristic nuclear time (10^{-20} s).[30] Therefore, it is reasonable to treat the decay-causing interaction in β decay as a weak perturbation. The essential features of β decay could be derived from the basic expression for the transition probability, which can be calculated by the time-dependent perturbation theory.[30,31] As discussed in Refs. [32–34] the non-exponential behavior also exists in the early time of β decay, and the time range where β decay process has a larger deviation from exponential decay law was also estimated. In Ref. [29] Kofman and Kurizki found that the modification of the decay rate is determined by the spectral density function (SDF) of the environment and the energy spread induced by the measurements, and the AZE in β decay was predicted by analyzing the SDF of the environment in β decay process. In Ref. [35] Giacosa and Pagliara deduced the expression of decay rate of neutron under frequency measurements and showed the acceleration effect of the measurements by the numerical results of decay rate. Moreover, by applying the AZE in the neutron decay, they addressed the issue of possible differences of the neutron lifetime that obtained by different experiments. The research of AZE in β decay will deepen the understanding of the

Supported by the National Natural Science Foundation of China (Grant Nos. 11822503 and 11575082), and the Fundamental Research Funds for the Central Universities (Nanjing University).

*Corresponding author. Email: cxu@nju.edu.cn

© 2021 Chinese Physical Society and IOP Publishing Ltd

peculiar quantum phenomenon of AZE, and it may be instructive to further explore the AZE in other decay processes. Thus the target of this study is to perform a detailed investigation of the AZE in the different types of β decay (namely, β^-, β^+ decay and EC) by the time-dependent perturbation theory. Furthermore, we show the effects of frequency measurements by the numerical results of decay rates of ^{3}H, ^{60}Co (β^- type), ^{22}Na, ^{106}Ag (β^+ type), ^{18}F, ^{57}Co and ^{111}Sn (EC type). The possible experimental candidate to observe AZE in nuclear β decay is also discussed.

The decay rate is the transition probability per unit time for the decay of a nucleus. The expression of decay probability can be deduced by the time-dependent perturbation theory. The Hamiltonian of the decay system is $\hat{H} = \hat{H}_0 + \hat{H}_{\rm int}$. Taking β^- decay as an example, we can find that a neutron exists in a nuclear state at time $t = 0$, and the eigenvector of initial state is denoted as $|n\rangle$, which is the eigenvector of $\hat{H}_0$ with eigenvalue $\hbar\omega_n$ and describes the Hilbert space form of the many-body wave function of parent nucleus. After decay, the neutron is changed into a proton by emitting an electron and an antineutrino.[36] Therefore, the eigenvector of final state, which can be written as $|e\bar{\nu}p\rangle$, includes the Hilbert space form of not only the many-body wave function of daughter nucleus, but also the wave functions of electron and antineutrino. The $|e\bar{\nu}p\rangle$ is orthogonal with $|n\rangle$ in the Hilbert space, and is also the eigenvector of $\hat{H}_0$ with eigenvalue $\hbar\omega_{e\bar{\nu}p}$. The interaction between $|n\rangle$ and $|e\bar{\nu}p\rangle$ can be written as $\hat{H}_{\rm int} = \sum_{e,\bar{\nu}}[H_{{\rm int}(e\bar{\nu}p,n)}|e\bar{\nu}p\rangle\langle n| + {\rm h.c.}]$, where $H_{{\rm int}(e\bar{\nu}p,n)} = \langle e\bar{\nu}p|\hat{H}_{\rm int}|n\rangle$. One can write the eigenvector of the decay system as $|\Psi(t)\rangle = \alpha(t)e^{-i\omega_n t}|n\rangle + \sum_{e,\bar{\nu}}\beta_{e\bar{\nu}}(t)e^{-i\omega_{e\bar{\nu}p}t}|e\bar{\nu}p\rangle$. According to the time-dependent Schrödinger equation $i\hbar[\partial|\Psi(t)\rangle/\partial t] = \hat{H}|\Psi(t)\rangle$, one can obtain

$$\dot{\alpha}(t) = -\frac{i}{\hbar}\sum_{e,\bar{\nu}} H_{{\rm int}(n,e\bar{\nu}p)}e^{i(\Delta\omega-\omega_{e\bar{\nu}})t}\beta_{e\bar{\nu}}(t), \quad (1)$$

$$\dot{\beta}_{e\bar{\nu}}(t) = -\frac{i}{\hbar}H_{{\rm int}(e\bar{\nu}p,n)}e^{-i(\Delta\omega-\omega_{e\bar{\nu}})t}\alpha(t), \quad (2)$$

where $H_{{\rm int}(n,e\bar{\nu}p)} = H^{\dagger}_{{\rm int}(e\bar{\nu}p,n)} = \langle n|\hat{H}_{\rm int}|e\bar{\nu}p\rangle$. $\Delta\omega = \Delta E/\hbar$, and ΔE represents the difference between the initial and final nuclear state energies, so the ΔE is equal to decay energy Q of β^- decay process. The Q equals the difference between the initial and final nuclear mass energies when the initial and final nuclei are in ground states.[30,31] In addition, for the case where the final nuclear state is in an excited state, the Q should be accordingly decreased by the excitation energy of the state.[30] Moreover, $\omega_{e\bar{\nu}} = E_{e\bar{\nu}}/\hbar$, where $E_{e\bar{\nu}}$ is the sum of electron and antineutrino relativistic kinetic energies (namely the maximum of relativistic kinetic energy of electron).[36] Combining Eqs. (1) and (2), we have

$$\dot{\alpha}(t) = -\sum_{e,\bar{\nu}}\frac{|H_{{\rm int}(n,e\bar{\nu}p)}|^2}{\hbar^2}\int_0^t e^{i(\Delta\omega-\omega_{e\bar{\nu}})(t-t')}\alpha(t')dt'. \quad (3)$$

Constrained by a sufficiently short time t, there appears to be $\alpha(t) \simeq \alpha(0) = 1$. Setting $\alpha(t') = 1$ on the right-hand side of Eq. (3) yields[29,37]

$$\alpha(t) \simeq 1 - \sum_{e,\bar{\nu}}\frac{|H_{{\rm int}(n,e\bar{\nu}p)}|^2}{\hbar^2}\int_0^t (t-t')e^{i(\Delta\omega-\omega_{e\bar{\nu}})t'}dt'. \quad (4)$$

If we perform n periodical measurements onto $|n\rangle$ with sufficiently small intervals τ, the survival probability of the $|n\rangle$ is

$$P(t = n\tau) = P^n(\tau) = \alpha^2(t) = \alpha^{2n}(\tau) = e^{-\lambda(\tau)t}, \quad (5)$$

where $\lambda(\tau)$ is effective decay rate. Setting $f(t) = (1 - t/\tau)e^{i\Delta\omega t}\theta(\tau - t)$ [step function $\theta(\tau - t)$ is 1 for $t < \tau$ and 0 for $t > \tau$] and inserting Eq. (4) into Eq. (5), one can reach

$$\begin{aligned}\lambda(\tau) &= -\frac{2}{\tau}\ln\alpha(\tau)\\ &\approx 2{\rm Re}\Big[\sum_{e,\bar{\nu}}\frac{|H_{{\rm int}(n,e\bar{\nu}p)}|^2}{\hbar^2}\int_0^{\tau}dt(1-\frac{t}{\tau})e^{i\Delta\omega t}e^{-i\omega_{e\bar{\nu}}t}\Big]\\ &= 2{\rm Re}\Big[\int_0^{\tau}dtf(t)\phi(t)\Big], \end{aligned} \quad (6)$$

where $\phi(t) = \sum_{e,\bar{\nu}}\hbar^{-2}|H_{{\rm int}(n,e\bar{\nu}p)}|^2e^{-i\omega_{e\bar{\nu}}t}$. Equation (6) can be recast by applying the SDF $G(\omega) = \sum_{e,\bar{\nu}}\hbar^{-2}|H_{{\rm int}(n,e\bar{\nu}p)}|^2\delta(\omega - \omega_{e\bar{\nu}})$, which is the Fourier transformation of $\phi(t)$, the effective decay rate is given by

$$\begin{aligned}\lambda(\tau) &= 2{\rm Re}\Big[\int_0^{\infty}dtf(t)\phi(t)\Big]\\ &\approx 2{\rm Re}\Big[\int_0^{\tau}dtf(t)\int_0^{\infty}d\omega G(\omega)e^{-i\omega t}\Big]\\ &= 2\pi\int_0^{\infty}F(\omega,\tau)G(\omega)d\omega, \end{aligned} \quad (7)$$

and the $F(\omega,\tau)$ is given by

$$F(\omega,\tau) = \frac{\tau}{2\pi}{\rm sinc}^2\Big[\frac{(\omega-\Delta\omega)\tau}{2}\Big], \quad (8)$$

which is the Fourier transformation of $f(t)$ and describes the effect of frequency measurements. Because the state $|e\bar{\nu}p\rangle$ is a spectrally dense band, the SDF should be rewritten as $G(\omega) = \sum_{e,\bar{\nu}}\hbar^{-1}|H_{{\rm int}(n,e\bar{\nu}p)}|^2\rho(\omega)$, and the $\rho(\omega)$ is the density of final state.[29] The $G(\omega)$ is then called the reservoir coupling spectrum function.[38]

The unstable states have an uncertain energy width Γ due to the energy-time uncertainty relation $\Gamma\cdot\tau \sim \hbar$. The measurement interval τ is a finite time

and therefore Γ is finite. As discussed in Ref. [35] the integration domain in Eq. (7) should also be finite. It is assumed that the integral range is $[\Delta\omega-\Lambda, \Delta\omega+\Lambda]$, if the $\Delta\omega-\Lambda<0$, the lower bound of the integration should be replaced by 0, and using ω_c, which is called the cut-off frequency and equals $\Delta\omega+\Lambda$, to denote the upper range of the integration, so one can rewrite Eq. (7) as

$$\lambda(\tau)=2\pi\int_0^{\omega_c}F(\omega,\tau)G(\omega)d\omega. \tag{9}$$

Thus, Eq. (9) shows that the effective decay rate is simply the overlap of the reservoir coupling spectrum function $G(\omega)$ and the measurement-induced level width function $F(\omega,\tau)$.[29] When the $\tau\to\infty$, namely no measurements within decay process, the 'golden rule' value (natural decay rate)

$$\lambda(\tau)=\lambda_0=2\pi G(\Delta\omega). \tag{10}$$

For the cases of β^+ decay and EC, the expression of the effective decay rates are identical with Eq. (13) using time-dependent perturbation theory.

For the function $F(\omega,\tau)$, the main lobe which ranges from $\Delta\omega-2\pi/\tau$ to $\Delta\omega+2\pi/\tau$ accounts for about 90.3% $[\int_{\Delta\omega-2\pi/\tau}^{\Delta\omega+2\pi/\tau}F(\omega,\tau)d\omega/\int_0^{\infty}F(\omega,\tau)d\omega=90.3\%]$ of the entire frequency domain.[37] As we can see from Fig. 1, when the difference between $\Delta\omega$ and the center of gravity of $G(\omega)$ is not extremely large [such as $G(\omega)\propto\omega^{\eta}$, where $0<\eta<1$], it is reasonable to replace the integral domain $[0,\omega_c]$ by $[\Delta\omega-2\pi/\tau,\Delta\omega+2\pi/\tau]$. Thus one can obtain[37]

$$\begin{aligned}\lambda(\tau)=&2\pi\int_{\Delta\omega-\frac{2\pi}{\tau}}^{\Delta\omega+\frac{2\pi}{\tau}}[G(\omega)-G(\Delta\omega)]F(\omega,\tau)d\omega\\&+2\pi G(\Delta\omega)\\=&\frac{2}{\tau}\int_{\Delta\omega-\frac{2\pi}{\tau}}^{\Delta\omega+\frac{2\pi}{\tau}}\Big[\Big(\sum_{n=0}\frac{G^{(n)}(\Delta\omega)}{n!}(\omega-\Delta\omega)^n\\&-G(\Delta\omega)\Big)\times\frac{1-\cos(\omega-\Delta\omega)\tau}{(\omega-\Delta\omega)^2}\Big]d\omega\\&+2\pi G(\Delta\omega)\\=&2\pi G(\Delta\omega)+\frac{4\pi}{\tau^2}G^{(2)}(\Delta\omega)+O(\tau^{-3})\\=&\lambda_0+\lambda_1(\tau),\end{aligned} \tag{11}$$

where $\lambda_1(\tau)=4\pi G^{(2)}(\Delta\omega)/\tau^2$.

On the contrary, if the $G(\omega)$ grows or declines faster in the whole integral domain [such as $G(\omega)\propto\omega^{\eta}$, where $\eta<0$ or $\eta>1$ (see Fig. 1)]. The integral domains $[0,\Delta\omega-2\pi/\tau]$ and $[\Delta\omega+2\pi/\tau,\omega_c]$ become non-negligible. In the integration over the minor lobes of $F(\omega,\tau)$, it is assumed that the value of the integration is insensitive to the oscillating behavior of $F(\omega,\tau)$, therefore one can use its mean value 1/2 to replace the square sine function, Eq. (8) could be rewritten as[37,39]

$$\begin{aligned}F(\omega,\tau)=&\frac{\tau}{2\pi}\frac{\sin^2[(\omega-\Delta\omega)\tau/2]}{[(\omega-\Delta\omega)\tau/2]^2}\\\approx&\frac{\tau}{2\pi}\frac{1/2}{[(\omega-\Delta\omega)\tau/2]^2}=\frac{1}{\pi\tau(\omega-\Delta\omega)^2}.\end{aligned} \tag{12}$$

If we assume $\lambda_2(\tau)=2\pi\int_0^{\Delta\omega-2\pi/\tau}F(\omega,\tau)[G(\omega)-G(\Delta\omega)]d\omega$ and $\lambda_3(\tau)=2\pi\int_{\Delta\omega+2\pi/\tau}^{\omega_c}F(\omega,\tau)[G(\omega)-G(\Delta\omega)]d\omega$, one can obtain

$$\begin{aligned}\lambda_2(\tau)=&\frac{2}{\tau}\int_0^{\Delta\omega-\frac{2\pi}{\tau}}\frac{G(\omega)-G(\Delta\omega)}{(\omega-\Delta\omega)^2}d\omega\\=&\frac{2}{\tau}\int_0^{\Delta\omega-\frac{2\pi}{\tau}}\frac{G(\omega)}{(\omega-\Delta\omega)^2}d\omega\\&-G(\Delta\omega)\Big(\frac{1}{\pi}-\frac{2}{\Delta\omega\tau}\Big),\end{aligned} \tag{13}$$

and

$$\begin{aligned}\lambda_3(\tau)=&\frac{2}{\tau}\int_{\Delta\omega+\frac{2\pi}{\tau}}^{\omega_c}\frac{G(\omega)-G(\Delta\omega)}{(\omega-\Delta\omega)^2}d\omega\\=&\frac{2}{\tau}\int_{\Delta\omega+\frac{2\pi}{\tau}}^{\omega_c}\frac{G(\omega)}{(\omega-\Delta\omega)^2}d\omega\\&-G(\Delta\omega)\Big[\frac{1}{\pi}-\frac{2}{(\omega_c-\Delta\omega)\tau}\Big],\end{aligned} \tag{14}$$

by applying Eq. (12). Therefore, if the whole domain from 0 to ω_c is considered in the integration, the $\lambda(\tau)=\lambda_0+\lambda_1(\tau)+\lambda_2(\tau)+\lambda_3(\tau)$. The magnitude of $\lambda(\tau)$ depends on the form of $G(\omega)$.

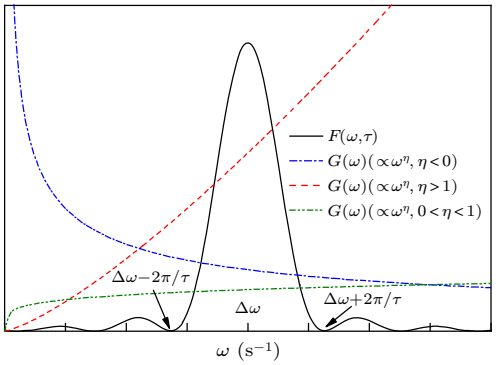

Fig. 1. Schematic of the overlaps between the different spectrum density functions $G(\omega)$ and $F(\omega,\tau)$.

In the cases of β^+ and β^- decay, we use a simplified formula for the $G(\omega)$ of the nucleon, namely the Sargent rule:[31,35]

$$G(\omega)=c_1\omega^5, \tag{15}$$

where the parameter c_1 contains the complex nuclear matrix elements part and ω^5 describes the dependence of decay constant on the decay energy in β^+/β^- decay. According to Eq. (10), the c_1 could be determined by $c_1=\frac{\lambda_0}{2\pi\Delta\omega^5}$. However, in practical calculations the parameter c_1 is canceled out in the ratio between the

effective decay rate and the natural one. By substituting Eq. (15) into Eqs. (11), (13) and (14), the explicit result of $\lambda(\tau)$ reads:

$$\lambda(\tau) = 2\pi G(\Delta\omega)\Big\{1 + \frac{1}{4\pi\tau\Delta\omega^5}\Big[\omega_c^4 + 2.67\omega_c^3\Delta\omega + 6\omega_c^2\Delta\omega^2 + 16\omega_c\Delta\omega^3 + 20\Delta\omega^4 \ln\Big(\frac{\omega_c}{\Delta\omega} - 1\Big)\Big]\Big\}. \tag{16}$$

From Eq. (16) it can be seen that, besides the measurement interval, the different values of ω_c also result in the different effective decay rates. The derivation of Eq. (16) is based on the integration in Eq. (9), where the lower bound of the integration is 0, therefore, the $\Delta\omega - \Lambda \leq 0$ and $\omega_c \geq 2\Delta\omega$. Moreover, the upper range of the value of ω_c should also be restricted. As discussed in Ref. [35] because Eq. (15) is valid up to the opening of the strong interaction threshold at $\omega = \Delta\omega + m_\pi c^2/\hbar$, where the m_π is the mass of pion, the value of $\omega_c \leq 10\Delta\omega$ ($10\Delta\omega < m_\pi c^2/\hbar$) is reasonable in our calculation. The numerical results of the ratio between effective decay rate and natural decay rate under different values of ω_c are shown in Fig. 2. The related data of the decay processes (such as half-lives, decay energies) are taken from Ref. [40].

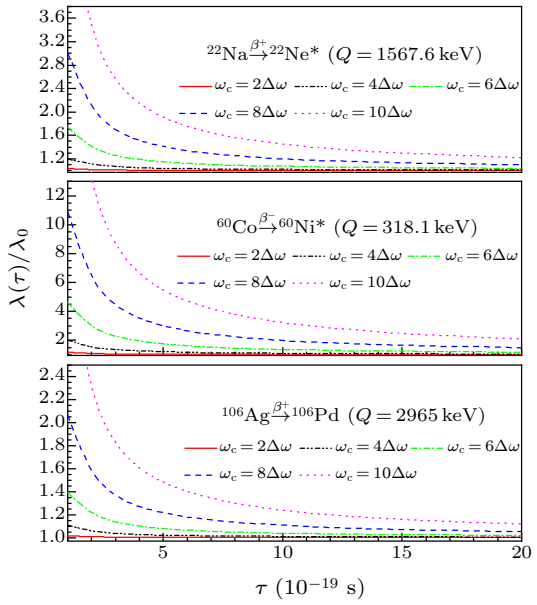

Fig. 2. Variations of the ratio between the effective decay rate and the natural one for the β^+ or β^- decay of ^{26}Al, ^{60}Co and ^{106}Ag under $\omega_c = 2, 4, 6, 8, 10\Delta\omega$. The symbol $*$ represents that final nucleus is in an excited state. The excitation energies of ^{22}Ne* and ^{60}Ni* are 1274.5 keV and 2505.8 keV, respectively. The branching ratios of the dominant decay channel of ^{22}Na, ^{60}Co, and ^{106}Ag are 99.962 %, 99.925 %, and 82.9 %, respectively.

In the case of EC, the SDF $G_{\rm EC}(\omega)$ can be expressed as[31]

$$G_{\rm EC}(\omega) = c_2\omega^2, \tag{17}$$

where c_2 could be determined by $c_2 = \frac{\lambda_0}{2\pi\Delta\omega^2}$ and ω^2 describes the dependence of decay constant on the decay energy in EC. Similarly, the parameter c_2 is also canceled out in the ratio between the effective decay rate and the natural one. By applying Eq. (17) into Eqs. (11), (13) and (14), the explicit result of $\lambda_{\rm EC}(\tau)$ reads

$$\lambda_{\rm EC}(\tau) = 2\pi G_{\rm EC}(\Delta\omega)\left[1 + \frac{\omega_c + 2\Delta\omega\ln(\frac{\omega_c}{\Delta\omega} - 1)}{\pi\tau\Delta\omega^2}\right]. \tag{18}$$

The restriction of the value of ω_c is identical with the cases of β^+ and β^- decay. The numerical results of $\lambda_{\rm EC}(\tau)/\lambda_0$ under different values of ω_c are shown in Fig. 3.

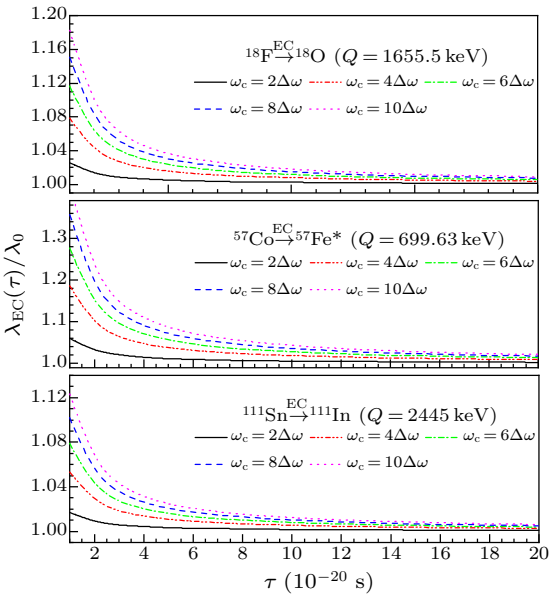

Fig. 3. Variations of the ratio between the effective decay rate and the natural one for the EC of ^{18}F, ^{57}Co, ^{111}Sn under $\omega_c = 2, 4, 6, 8, 10\Delta\omega$. The excitation energy of ^{57}Fe* is 136.5 keV. The ^{18}F has only one decay channel, and the branching ratios of the dominant decay channel of ^{57}Co and ^{111}Sn are 99.8 % and 91.2 %, respectively.

By inserting $\omega_c = k\Delta\omega$ ($k = 2, 4, 6, 8, 10$ in this study) into Eqs. (16) and (18), one can obtain $\lambda(\tau) = \lambda_0[1 + \frac{k^4+2.67k^3+6k^2+16k+20ln(k-1)}{4\pi(\tau\cdot\Delta\omega)}]$ and $\lambda_{\rm EC}(\tau) = \lambda_0[1 + \frac{k+2\ln(k-1)}{\pi(\tau\cdot\Delta\omega)}]$. Therefore, if we consider the fixed values of $\lambda(\tau)/\lambda_0$ [or $\lambda_{\rm EC}(\tau)/\lambda_0$] and ω_c, the product of $\Delta\omega$ and τ would be a constant in Eqs. (16) and (18). A lager measurement interval is favorable to observe the AZE in experiment, so the experimental candidates of nucleus should have a smaller decay energy. From Figs. 2 and 3, it can be seen that the values of measurement intervals, which are required to obtain a sizable AZE [10% AZE: $\lambda(\tau)$ or $\lambda_{\rm EC}(\tau) = 1.1\lambda_0$] in the cases of β^+, β^- decay and EC, are of the orders of 10^{-18} s and 10^{-20} s, respectively, when $\omega_c = 8\Delta\omega$. Therefore it can be known that the frequency measurements have a more obvious acceleration effect on the decay rates of β^+ and β^- compared with EC under

identical measurement interval and cut-off frequency, and the experimental candidates should be selected from the nuclei with decay type β^+ or β^-. Moreover, a reasonable half-life of candidates should also be considered for the experimental manipulation. We take the β^- decay of ^{3}H as an example, its decay energy is 18.6 keV, which is the smallest in all β decay nuclei, and its half-life is 12.33 yr. Thus ^{3}H may be a suitable experimental candidate to observe the AZE in β decay. The numerical results of the ratio between effective decay rate and natural decay rate under different values of ω_c are shown in Fig. 4. It can be seen that the measurement interval, which is required to observe a sizable AZE in experiment, is of the order of 10^{-16} s when $\omega_c = 8\Delta\omega$.

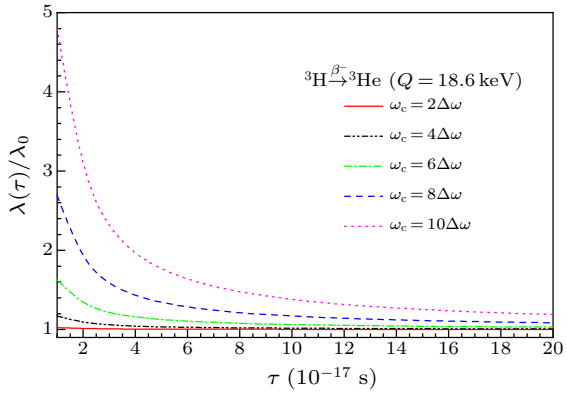

Fig. 4. Variations of the ratio between effective decay rate and the natural one for the β^- decay of ^{3}H under $\omega_c = 2, 4, 6, 8, 10\Delta\omega$. The ^{3}H only has one decay channel.

We have investigated the AZE in seven nuclei ^{3}H, ^{18}F, ^{22}Na, ^{57}Co, ^{60}Co, ^{106}Ag, and ^{111}Sn. The reasons for choosing these nuclei are as follows: Firstly, all of these unstable nuclei are 100 % β decay. For ^{3}H and ^{18}F, there is only one β decay channel (ground state to ground state). For the remaining nuclei, multi β decay channels exist but the branching ratio of the dominant one is larger than 80 %. Secondly, the decay half-lives of these nuclei, ranging from 23.96 min to 12.33 yr, are within the capability of experiments.

It is clear that the AZE dominates in all types of β decay under frequency measurements, so it is necessary to discuss the reason why the QZE is excluded in β decay. From Eq. (8) we can see $F(\omega, \tau \to 0) = 0$, and therefore

$$\lambda(\tau \to 0) = 2\pi \int_0^{\omega_c} F(\omega, \tau \to 0) G(\omega) d\omega = 0. \quad (19)$$

As discussed in Ref. [35] in order for Eq. (19) to apply, one needs a very large and unrealistic value of the cut-off frequency ω_c of the order of GUT (grand unified theory) scale to ensure that the SDF still has an overlap with $F(\omega, \tau)$ at the large ω_c (because the width of $F(\omega, \tau)$ will approach ∞ when $\tau \to 0$), but this is far beyond the applicable range of Eqs. (15) and (17). Moreover, such a small measurement interval is very difficult to achieve in the experiment. Therefore, the discussion shows that QZE is extremely difficult to be observed in β decay.

In summary, we have investigated the quantum anti-Zeno effect (AZE) in nuclear β decay. The expression of β decay rate under frequency measurements is derived from the time-dependent perturbation theory. By calculating the decay rates of nuclei from different types of β decay, it is found that the values of measurement intervals to observe a sizable AZE (namely, 10% AZE) in β^+, β^- decay and EC are of the order of 10^{-18} s and 10^{-20} s, respectively, when $\omega_c = 8\Delta\omega$. Therefore the acceleration effects by frequency measurements for the cases of β^- and β^+ decay are more obvious than the case of EC under identical measurement interval and cut-off frequency. For example, when the measurement intervals is 10^{-20} s, the values of the ratio $\lambda(\tau)/\lambda_0$ of ^{106}Ag (β^+ type) is 10.58 times larger than the value of the ratio $\lambda_{\mathrm{EC}}(\tau)/\lambda_0$ of ^{111}Sn (EC type) under $\omega_c = 8\Delta\omega$. Furthermore, the expression of the effective decay rate shows that a small decay energy is favorable to observe the AZE in experiment. Therefore, we suggest ^{3}H, with the smallest β^- decay energy 18.6 keV, as one possible experimental candidate to observe the AZE in β decay. By the calculation of AZE in the decay of ^{3}H, the effective decay rate of ^{3}H is 2.69 times larger than the natural decay rate when the measurement interval is 10^{-17} s, and the smallest measurement interval that must be achieved to observe a sizable AZE is of the order of 10^{-16} s when $\omega_c = 8\Delta\omega$.

References

[1] Wilkinson S R, Bharucha C F, Fischer M C, Madison K W, Morrow P R, Niu Q, Sundaram B and Raizen M G 1997 *Nature* **387** 575
[2] Grotz K and Klapdor H V 1984 *Phys. Rev. C* **30** 2098
[3] Chiu C B and Sudarshan E C G 1977 *Phys. Rev. D* **16** 520
[4] Fonda L, Ghirardi G C and Rimini A 1978 *Rep. Prog. Phys.* **41** 587
[5] Panov A D 1999 *Phys. Lett. A* **260** 441
[6] Itano W M, Heinzen D J, Bollinger J J and Wineland D J 1990 *Phys. Rev. A* **41** 2295
[7] Home D and Whitaker M A B 1997 *Ann. Phys.* **258** 237
[8] Segal D and Reichman D R 2007 *Phys. Rev. A* **76** 012109
[9] Misra B and Sudarshan E C G 1977 *J. Math. Phys. (N. Y.)* **18** 756
[10] Goto H and Ichimura K 2008 *Phys. Rev. A* **78** 044102
[11] Koshino K and Shimizu A 2005 *Phys. Rep.* **412** 191
[12] Zhang X, Xu C, Ren Z Z and Peng J 2018 *Sci. Rep.* **8** 10267
[13] Erez N, Gordon G, Nest M and Kurizki G 2008 *Nature* **452** 724
[14] Barenco A, Berthiaume A, Deutsch D, Ekert A, Jozsa R and Macchiavello C 1997 *SIAM J. Comput.* **26** 1541
[15] Maniscalco S, Francica F, Zaffino R L, Lo G N and Plastina F 2008 *Phys. Rev. Lett.* **100** 090503
[16] Wang X B, You J Q and Nori F 2008 *Phys. Rev. A* **77** 062339

[17] Maniscalco S, Piilo J and Suominen K A 2006 *Phys. Rev. Lett.* **97** 130402
[18] Yang Y, Fleischhauer M and Zhu S Y 2003 *Phys. Rev. A* **68** 022103
[19] Zheng H, Zhu S Y and Zubairy M S 2008 *Phys. Rev. Lett.* **101** 200404
[20] Block E and Berman P R 1991 *Phys. Rev. A* **44** 1466
[21] Sabín C, León J and Garcíjua-Ripoll J J 2011 *Phys. Rev. B* **84** 024516
[22] Lewenstein M and Rzażewski K 2000 *Phys. Rev. A* **61** 022105
[23] Streed E W, Mun J, Boyd M, Campbell G K, Medley P, Ketterle W and Pritchard D E 2006 *Phys. Rev. Lett.* **97** 260402
[24] Wolters J, Strau M, Schoenfeld R S and Benson O 2013 *Phys. Rev. A* **88** 020101
[25] Zheng W, Xu D Z, Peng X, Zhou X, Du J and Sun C P 2013 *Phys. Rev. A* **87** 032112
[26] Kalb N, Cramer J, Twitchen D J, Markham M, Hanson R and Taminiau T H 2016 *Nat. Commun.* **7** 13111
[27] Fischer M C, Gutiérrez-Medina B and Raizen M G 2001 *Phys. Rev. Lett.* **87** 040402
[28] Chen P W, Tsai D B and Bennett P 2010 *Phys. Rev. B* **81** 115307
[29] Kofman A G and Kurizki G 2000 *Nature* **405** 546
[30] Krane K S 1989 *Introductory Nuclear Physics* (New York: John Wiley *&* Sons Ins Press) unit II chap 9 p **274** 277
[31] Heyde K 1999 *Basic Ideas and Concepts in Nuclear Physics* (Bristol: IOP Publishing) part B chap 5 p 118
[32] Ray A and Sikdar A K 2016 *Phys. Rev. C* **94** 055503
[33] Norman E B and Gazes S B 1988 *Phys. Rev. Lett.* **60** 2246
[34] Avignone F T 1988 *Phys. Rev. Lett.* **61** 2624
[35] Giacosa F and Pagliara G 2020 *Phys. Rev. D* **101** 056003
[36] Wilson F L 1968 *Am. J. Phys.* **36** 1150
[37] Zhang J M, Jing J, Wang L G and Zhu S Y 2018 *Phys. Rev. A* **98** 012135
[38] Kofman A G and Kurizki G 2001 *Phys. Rev. Lett.* **87** 270405
[39] Lassalle E, Champenois C, Stout B, Debierre V and Durt T 2018 *Phys. Rev. A* **97** 062122
[40] Firestone R B 1996 *Table of Isotopes* 8th edn (New York: Wiley InterScience) pp 254, 388, 456, 1333, 1423, 3218, 3459